Biomaterials 31 (2010) 1604–1611

Contents lists available at ScienceDirect

Biomaterials

journal homepage: www.elsevier.com/locate/biomaterials

The use of immobilized osteogenic growth peptide on gradient substrates synthesized via click chemistry to enhance MC3T3-E1 osteoblast proliferation

Nicole M. Moore [a], Nancy J. Lin [a], Nathan D. Gallant [a], Matthew L. Becker [a,b,*]

[a] Polymers Division, National Institute of Standards and Technology, Gatihersburg, MD 20899-8543, USA
[b] Department of Polymer Science, University of Akron, Akron, OH 44325-3909, USA

ARTICLE INFO

Article history:
Received 26 August 2009
Accepted 3 November 2009
Available online 22 November 2009

Keywords:
Bone tissue engineering
Osteoblast
Peptide
Cell proliferation

ABSTRACT

In this study, we report the use of surface immobilized peptide concentration gradient technology to characterize MC3T3-E1 osteoblast cell response to osteogenic growth peptide (OGP), a small peptide found naturally in human serum at μmol/L concentrations. OGP was coupled to oxidized self assembled monolayer (SAM) gradients by a polyethylene oxide (PEO) linker using click chemistry. After 4 h incubation with MC3T3-E1 cells, OGP functionalized surfaces had higher cell attachment at low peptide concentrations compared to control gradients. By day 3, OGP gradient substrates had higher cell densities compared to control gradients at all concentrations. MC3T3-E1 cell doubling time was 35% faster on OGP substrates relative to SAM gradients alone, signifying an appreciable increase in cell proliferation. This increase in cell proliferation, or decrease in doubling time, due to OGP peptide was reduced by day 7. Hence, immobilized OGP increased cell proliferation from 0 days to 3 days at all densities indicating it may be useful as a proliferative peptide that can be used in tissue engineering substrates.

1. Introduction

Over the past 15 years, significant efforts have focused on the development of biomimetic surfaces to stimulate tissue regeneration for treatment of bone defects. The aim of this research is to develop a biomimetic environment to induce one or more of the three stages of bone regeneration: cell proliferation, matrix maturation, and mineralization. However, rational development of microenvironments that promote cell proliferation and matrix mineralization requires an in depth understanding of complex cell–material interactions [1,2]. While many of the individual components and steps in the osteogenic processes have been identified, more research is needed to identify favorable spatial arrangements and density of immobilized bioactive ligand, such as growth factors and extracellular matrix (ECM) proteins that encourage cell proliferation and expression of matrix proteins [3,4].

One such ligand is osteogenic growth peptide (OGP), a short, naturally occurring 14-mer growth factor peptide found in serum at μmol/L concentrations [5,6]. As a soluble peptide, OGP regulates proliferation, differentiation, and matrix mineralization in osteoblast lineage cells [6,7]. The active portion of OGP, the OGP(10-14) region, is cleaved from the peptide and binds to the OGP receptor which activates the MAP kinase, the Src, and the RhoA pathways [8–10]. Activation of the MAP kinase pathway typically triggers increased mitogenic activity [11]. Src and RhoA pathways regulate the autocrine expression of endogenous OGP from osteoblast lineage cells [9]. When administered intravenously to animals, OGP and OGP(10-14) promote increased bone density and stimulate healing suggesting a potential use in bone tissue engineering applications [12].

Previous studies have demonstrated sensitivity of osteoblast lineage cells to changes in exogenous concentrations of OGP. Biphasic dependences have been observed in cell proliferation relative to OGP concentration due to the auto-regulation of endogenous OGP by the cells [6,8]. Studies investigating soluble OGP found that there is an optimal concentration (10^{-6} μmol/L to 10^{-7} μmol/L) of OGP needed to increase cell proliferation of osteoblast lineage cells [6,13]. In these studies the proliferative effect was observed after 48–72 h incubation with OGP.

For most tissue engineering applications, immobilized OGP is more practical than soluble OGP for maintaining tight spatial proximity with the cells at the wound site for extended periods of time. To date, only a few groups have examined the effectiveness of OGP incorporated into tissue engineered scaffolds. In these studies, OGP was incorporated into peptide nanofiber scaffolds or PLGA gels [14,15] and both found that OGP increased cell density compared to control substrates, demonstrating OGP use as an immobilized peptide. However, neither of these groups was able to determine

* Corresponding author. Department of Polymer Science, University of Akron, Akron, OH 44325-3909.
E-mail address: becker@uakron.edu (M.L. Becker).

0142-9612/$ – see front matter © 2009 Elsevier Ltd. All rights reserved.
doi:10.1016/j.biomaterials.2009.11.011

the density of immobilized OGP in the substrate, what fraction was bio-available or the effect that the immobilized OGP concentration had on the cell response.

Numerous strategies have been reported for the covalent attachment of peptides to surfaces [16]. These include more traditional amidation and esterification reactions but challenges associated with regiospecificity have led to new chemistries that are orthogonal to the functional groups found in naturally occurring amino acids. Orthogonal chemistries which broadly fall under the heading of click reactions are particularly useful for immobilizing peptides and have become increasingly powerful in biological chemistry due to broad utility in aqueous solution [17]. Immobilization strategies have included cycloaddition reactions especially Diels–Alder [18], 1,3-dipolar cycloaddition reactions, [19] and carbonyl chemistry including the formation of thioureas,[20] and oxime [21] ethers, among others.

We hypothesized that osteoblast lineage cells are sensitive to immobilized OGP concentration, therefore we have utilized a platform technology which affords a peptide concentration gradient of immobilized OGP [19]. These click functionalized universal substrates have been used previously to characterize RGD peptide interaction with smooth muscle cells. Using the gradients, it was determined that cell adhesion and cell spread area were influenced by the density of immobilized RGD peptide [19]. In this study, universal substrates were used to explore the effect of immobilized OGP and OGP(10-14) densities on pre-osteoblast cell adhesion, morphology, and proliferation.

2. Materials and methods

2.1. Materials[1]

Unless listed otherwise, all solvents and reagents were purchased from Sigma–Aldrich (St. Louis, MO) and used as received. Fmoc-protected amino acids and preloaded Wang-resins were purchased from Novabiochem (San Diego, CA). Alpha minimum essential medium (αMEM) and ultra culture media were purchased from Lonza; all other cell culture reagents were purchased from Invitrogen Corp. All reagents were used as-received.

2.2. Azo-peptide synthesis

OGP (Br-ALKRQGRTLYGFGG) and OGP(10-14) (Br-YGFGG) were synthesized with an Apex 396 peptide synthesizer (Aapptec, Louisville, KY) using standard solid phase FMOC chemistry. Bromohexanoic acid was coupled to the N-terminus of each peptide during synthesis. Peptides were cleaved from resin using standard conditions (2 h, 95% trifluoroacetic acid (TFA), 5% Triisopropylsilane (TIPS), 5% water (by volume)) and precipitated in diethyl ether. Following two trituration cycles, the peptides were dialyzed in deionized water (molecular weight (MW) cutoff 100 g/mol, cellulose membrane, Pierce), and molecular weight was verified with matrix assisted laser desorption ionization – time of flight (MALDI-TOF). (MW (OGP) = 1625.87 g/mol, MW (OGP(10-14)) = 601.65 g/mol).

Br terminated peptides were derivatized with sodium azide (1:5 molar ratio) and 18-crown-6 (mmol) in dimethylsulfoxide (DMSO) at 50 °C overnight. Product was vacuum dried, dialyzed against water (MW cutoff 100 g/mol, cellulose ester) (Pierce), and lyophilized. Product was verified with MALDI-TOF. (MW (OGP) = 1662.87 g/mol, MW (OGP(10-14)) = 638.65 g/mol).

2.3. Preparation of bifunctional polyethylene oxide (PEO) linker

2,2′-(Ethylenedioxy)bis(ethylamine) (5.00 g, 4.94 mL, 3.37×10^{-2} mol) was dissolved in 250 mL 1,4 dioxane and 50 mL of pyridine. Glycidyl propargyl ether (4.16 g, 4.00 mL, 3.71×10^{-2} mol) was added dropwise to the solution over a 1 h period at ambient temperature. The mixture was left to stir for 24 h. Deionized water (200 mL) was added to the solution and the solution was extracted 3 times in 100 mL of dichloromethane (DCM). The combined DCM extractions were dried overnight with $MgSO_4$ and concentrated.

[1] Certain equipment, instruments or materials are identified in this paper in order to adequately specify the experimental details. Such identification does not imply recommendation by the National Institute of Standards and Technology nor does it imply the materials are necessarily the best available for the purpose.

2.4. Gradient fabrication

Glass coverslips (24 mm × 60 mm) were ultraviolet ozone (UVO) treated for 30 min, rinsed with ethanol, and dried with nitrogen gas. Octyldimethylchlorosilane (ODMS) self assembled monolayer (SAM) was formed on glass coverslips by vapor deposition for 48 h. SAM formation was verified by advancing water contact angle measurements (DSP100, Kruss, Hamburg, Germany). To form the initial gradient, SAM substrates were treated with increasing exposure times of UVO (90–120 s) over a 40 mm distance using an automated system described previously [19].

SAM gradient surfaces were reacted with the bifunctional PEO linker as described previously [19]. SAM gradient surfaces were submerged in 30 mL of DCM, 100 mg of dimethylaminopyridine (DMAP), 1 mL of diisopropylcarbodiimide (DIC), and 150 mg of the bifunctional linker prepared as described above. Gradient surfaces were incubated and mixed in this solution for 24 h at 40 °C. Gradients were removed from the DCM solution, rinsed with methanol twice, and dried with N_2 gas yielding an alkyne derivatized surface. OGP and OGP(10-14) peptides were reacted with the alkyne gradients to form peptide gradient substrates via click chemistry.

To react peptide with linker gradient substrates, a 30 mL solution of 1:6 DMSO: water containing Cu(II)SO_4 (149.8 mg), sodium ascorbate (237.7 mg), and 5 mg of peptide was mixed together in a slide chamber. Linker gradient substrates were submerged in the solution, mixed thoroughly, and incubated for 24 h at 40 °C. Gradients were rinsed with deionized (DI) water and transferred to a slide chamber containing ethylenediaminetetraacetic acid (ETDA) (150 mg) in 30 mL of DI water. The gradients were incubated and mixed in the EDTA solution for 24 h. To block non-specific interactions, gradient substrates were incubated in 5% Pluronic 78 (by weight) in water for 24 h. Slides were rinsed with methanol and water and blown dry with N_2 gas. To sterilize gradient substrates for cell culture, gradients were submerged in 70% ethanol (by volume) in water for 20 min.

2.5. Contact angle measurements

Gradient substrate fabrication was verified by measuring the advancing contact angle of water and methylene iodide at 5 mm intervals on the surfaces. Using a drop shape analysis system (DSP 100, Kruss, Germany), 2 μL of water or methylene iodide were dispensed onto the surface at 25 °C and the contact angle was measured. Substrate surface energy, the sum of polar and dispersive free energy components, was determined by solving the equilibrium interfacial interaction equation for both liquids simultaneously [20]. The standard uncertainty of the contact angle measurement at each point along the gradient was determined by the standard deviation between three independent measurements per distance on three samples prepared under identical conditions.

2.6. X-ray photoelectron spectroscopy (XPS)

XPS measurements were performed by a Kratos AXIS Ultra DLS spectrometer. The X-ray source was monochromated aluminum, scanning over a binding-energy range of 0–1100 eV with a dwell time of 100 ms. Each spectrum was collected over a 300 μm × 700 μm sample area. The analyzer pass energy was 40 eV for C1s, N1s, and O1s scans. Peak areas were fit using a Levenberg–Marquardt algorithm assuming a linear background. For each gradient substrate fabrication step, the expected ratios of nitrogen to carbon were determined for a single ODMS molecule. For any given substrate position the percentage of alkylsilane sites reacted with peptide was calculated by determining the local ratio of nitrogen to carbon. Finally, the molar concentration of peptide as a function of substrate position was determined by assuming an alkylsilane brush density of 437 pmol/cm^2 [21].

2.7. Cell culture and characterization

MC3T3-E1 cells (Riken Cell Bank, Hirosaka, Japan) were cultured in α-MEM media (Lonza) supplemented with 10% (by volume) fetal bovine serum (FBS), 5 mmol/L L-glutamine, 100 units/mL penicillin, and 100 μg/mL streptomycin (PS) and incubated at 37 °C with 5% CO_2. For experiments, cells were seeded on gradient substrates at 25 cells/mm^2 in no serum ultra culture media and incubated for 4 h, 3 days, or 7 days at 37 °C and 5% CO_2. For each time point, cells were fixed and permeabilized (3.7% (by volume) formaldehyde, 0.5% (by volume) Triton-X, 3% bovine serum albumin (BSA) in 1× phosphate buffered saline (PBS) for 5 min, followed by 20 min incubation with 3.7% formaldehyde, 3% BSA, in PBS). The nuclei and cell bodies of fixed cells were stained with Hoechst 33342 (1 μg/mL in PBS, nucleus) and Texas red C2 maleimide (1 μmol/L dilution in PBS, cell body) for 1 h at 37 °C. Substrates were mounted onto glass slides with gel mount (Fisher Scientific).

Cell density, area, aspect ratio, and roundness were determined by automated fluorescence microscopy with a Leica DMR 1200 upright microscope equipped with a computer-controlled translation stage (Vashaw Scientific, Inc. Frederick, MD). Image Pro software (Media Cybernetics, Silver Spring, MD) controlled the stage and image acquisition. Gradients were imaged in a 5 × 20 grid, where 5 images were collected perpendicular to the gradient every 2 mm. Two fluorescent images were collected at each position, 360 nm excitation/470 nm emission and 560 nm excitation/645 nm emission. The 560 nm excitation images captured Texas red maleimide stain and were used to determine cell area, aspect ratio, and roundness. The 360 nm

Table 1
Primers used for real-time RT-PCR.

Gene	Protein	Left primer (5′–3′)	Right primer (5′–3′)
18 S	Ribosomal subunit	AGCGACCAAAGGAACCATAA	CTCCTCCTCCTCCTCTCTCG
Col1a1	Procollagen, type I, alpha 1	CTTCACCTACAGCACCCTTG	TTGGTGGTTTTGTATTCGATGA
Runx2	runt related transcription factor 2	ATGCCTCCGCTGTTATGAA	AGGTGAAACTCTTGCCTCGT

excitation images captured the Hoechst stain and were used to determine cell density. Each captured image had an area of 0.36 mm^2. A minimum of 3 gradient substrates was analyzed per group ($n = 3$). Data sets from every 2 mm intervals were binned into 4 mm intervals for data analysis.

2.8. Quantitative real-time reverse transcription polymerase chain reaction (RT-PCR)

MC3T3-E1 cells were cultured in no serum ultra culture media (Lonza) with and without 10^{-7} mol/L OGP or OGP(10-14) for 3 days and 7 days. For positive control, MC3T3-E1 cells were cultured in mineralizing media (αMEM media supplemented with 10 nmol/L dexamethasone, 20 mmol/L β-glycerolphosphate, 50 μmol/L L-ascorbic acid) for 3 days and 7 days. Cells were lysed with lysis buffer supplied in the RNeasy Mini Kit (Qiagen, Valencia, CA). Cell lysates were homogenized with a QIAshredder spin column (Qiagen), and RNA was harvested with the RNeasy Mini Kit and protocol (Qiagen). The isolated total RNA was quantified by absorbance at 260 nm using a Nanodrop Spectrophotometer (ND-1000, Thermo Fisher Scientific, Waltham, MA). Quantitative real-time RT-PCR was carried out on an iCycler (Biorad, Hercules, CA) using the QuantiTect SYBR Green RT-PCR kit and protocol. For each reaction, 200 ng of RNA template was used. Primers are listed in Table 1. The 18 S ribosomal subunit served as the internal reference. The thermal protocol consisted of reverse transcription at 50 °C for 30 min, activation at 95 °C for 15 min, and 50 amplification cycles (denaturation for 30 s at 95 °C, annealing for 1.5 min at 58 °C, and extension for 2 min at 72 °C). A melt curve, increasing in 1 °C temperature increments from 50 °C to 95 °C, was performed following amplification to analyze products generated. Additionally electrophoresis on 2% (by mass) agarose gels was used to analyze products. Standards were prepared for each gene as previously described [22]. Copy number of runx2 and collagen I mRNA was calculated from the threshold cycle for each sample using a standard curve and normalizing to the 18 S reference.

2.9. Statistics

Statistical analysis was performed using one-way analysis of variance (ANOVA) and a comparison-wise Tukey test at 95% confidence. Mean values and standard deviation are reported, unless otherwise noted. The standard deviations of the mean were used as an estimate for the standard uncertainty associated with each measurement technique.

3. Results

3.1. Immobilized OGP gradient substrate fabrication

OGP peptide and the C-terminus fragment of the peptide, OGP(10-14), were coupled to universal substrate gradients for high throughput analysis of cell response to immobilized peptide concentration [19]. Substrate gradients were fabricated on an ODMS

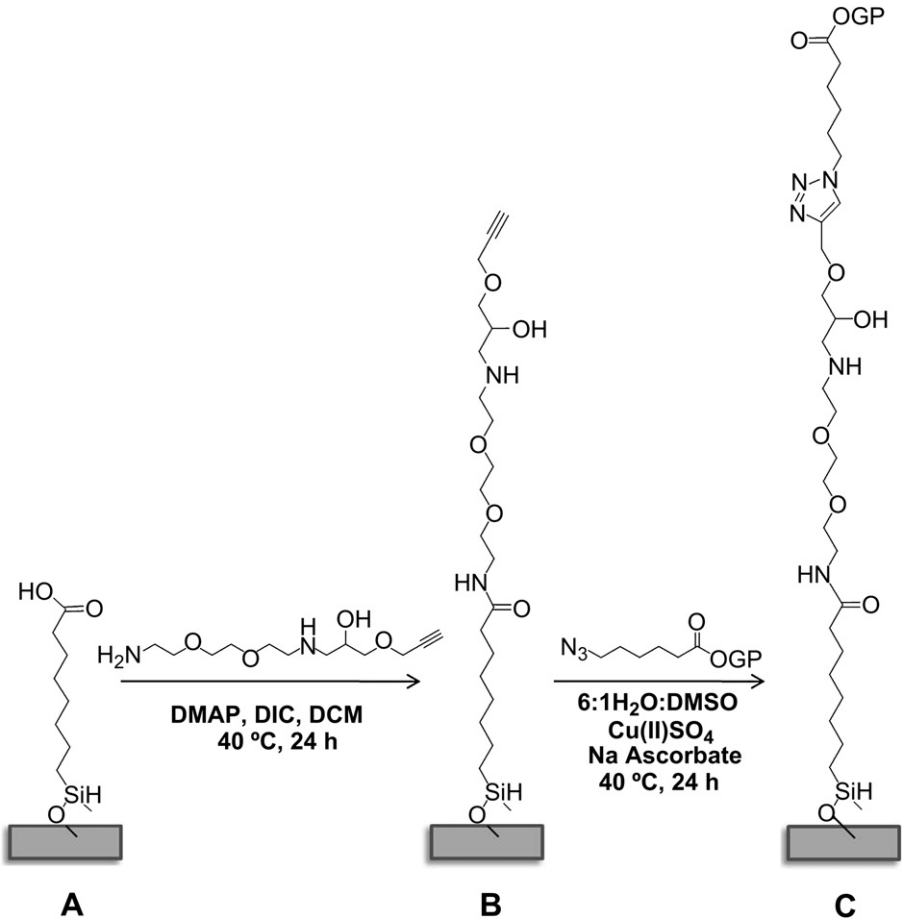

Fig. 1. Reaction scheme for coupling OGP peptide to UV oxidized SAM gradient substrates via click chemisty. (A) Carboxylic acid terminated SAMs are converted to (B) alkyne terminated SAM by coupling a difunctional PEG linker to the carboxylic acid group. (C) An azide terminated OGP peptide is covalently immobilized to the alkyne functionalized SAM by triazole cycloaddition. DMAP: 4-methylaminopyridine; DIC: diisopropylcarbodiimide; DMSO: dimethylsulfoxide; DCM: dichloromethane.

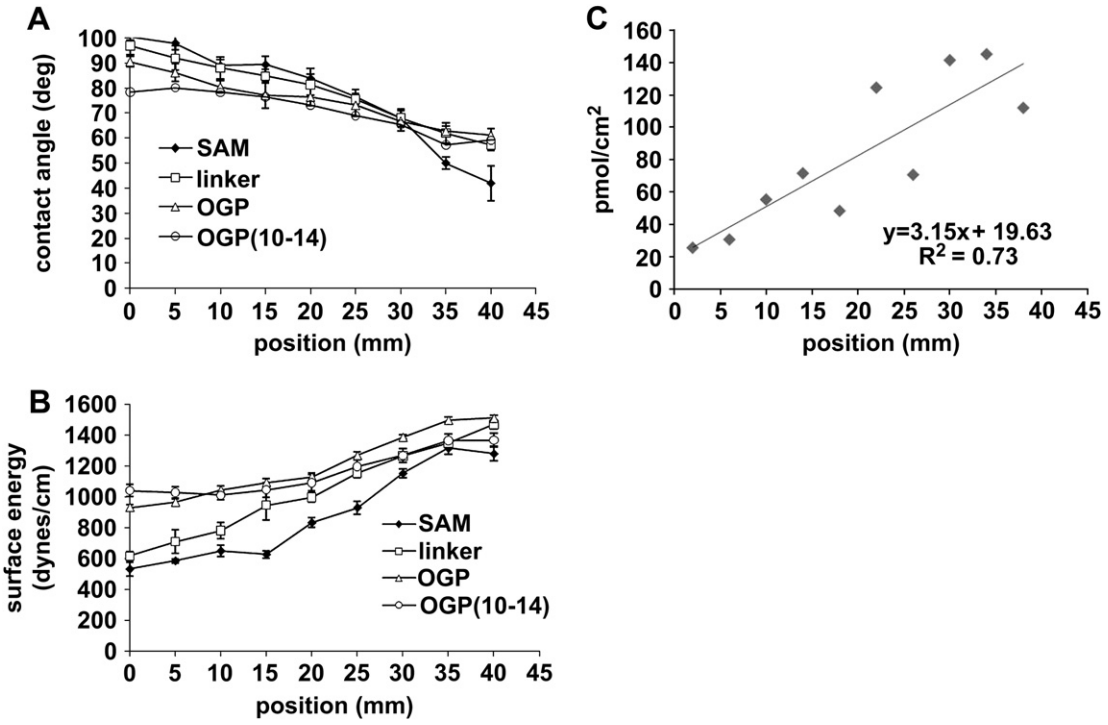

Fig. 2. Surface energy and peptide concentration vary as a function of position across the gradient surface. (A) Advancing water contact angles measured for each step of the substrate fabrication (B) Surface energies calculated by the advancing contact angles of deionized water and methylene iodide (C) Surface conjugated peptide density determined by XPS. Error bars reflect standard deviation.

SAM layer, that was exposed to increasing UVO exposure times resulting in a linear gradient of oxygen terminated SAM containing carboxylic acid, alcohols, and aldehyde functional groups. To form a peptide gradient, carboxylic functional groups (Fig. 1A) were reacted with the amine end of a heterobifunctional PEO linker, resulting in a linear gradient of alkyne groups (Fig. 1B). Azide terminated OGP or OGP(10-14) peptides were reacted to the alkyne gradient by click chemistry (Fig. 1C). The reaction was fast and specific resulting in consistent fabrication of peptide gradient substrates.

3.2. Gradient substrate characterization

Immobilized peptide gradient substrates were characterized by both advancing contact angle and XPS during each step in the fabrication. Advancing water and methylene iodide contact angles were used to measure the hydrophilicity and surface energy at each stage in the fabrication process to validate the presence of a gradient with increasing hydrophilicity and energy over 40 mm. Water contact angles on substrates at each step in the fabrication (i.e. SAM, linker, and peptide substrates) decreased 40°–50° over the length of the substrate (0 mm–40 mm). (Fig. 2A) Surface energies, determined from both water and methylene iodide advancing contact angles, increased on average ≈400 dyne/cm, ranging from 600 dyne/cm to 1400 dyne/cm over the length of the gradient. (Fig. 2B) Coupling the linker to the SAM gradient increased the average surface energy at every position on the substrate. Coupling peptide to the linker gradient increased surface energies further between 0 mm and 15 mm positions. These advancing contact angles demonstrate successful fabrication of gradient surfaces.

XPS measurements were performed in addition to contact angle measurements to verify OGP peptide gradients. XPS measures the elemental concentrations at each position on the gradient, providing more information on peptide concentration than contact angle. Correlation of XPS data to peptide molar concentration demonstrated that at the hydrophilic end of the scaffold approximately 40% of the alkylsilanes were reacted with peptide. This corresponds to a high peptide density of 140 pmol/cm^2. The range of peptide concentration on the substrate ranged from 0 pmol/cm^2 to 140 pmol/cm^2 (Fig. 2C).

3.3. Effect of immobilized OGP concentration on cell adhesion and morphology

Cell adhesion and morphology of MC3T3-E1 cells were measured on OGP and OGP(10-14) functionalized gradient surfaces. The cells were cultured in serum-free conditions to measure the direct impact of immobilized peptide on cell adhesion. To quantify cell adhesion versus peptide density, cells were seeded on gradient surfaces for 4 h, fixed, stained, and analyzed with automated microscopy. Analysis of the images demonstrated that at low peptide density (40 pmol/cm^2 to 60 pmol/cm^2), OGP functionalized surfaces had the highest cell density (2980 cell/cm^2) compared to OGP(10-14), PEO linker, and SAM gradient substrates. (Fig. 3A) Representative images of cells grown on these gradients at 50 pmol/cm^2 demonstrate visually the increase in cell adhesion at low OGP immobilized peptide concentration compared to SAM, PEO linker, and OGP(10-14) surfaces (Fig. 3B).

At high peptide density (60 pmol/cm^2 to 130 pmol/cm^2), the number of cells attached to OGP substrates decreased to an average of 2400 cells/cm^2, and the number of cells on PEO linker substrates increased to an average 3175 cells/cm^2. Cell density at 4 h on gradients coupled with the active portion of OGP, OGP(10-14), were similar to the cell density found on SAM gradients at all peptide concentrations, but did increase slightly with peptide concentration over the gradient. For all substrates, the number of cells on the substrates decreased at the end of the gradient (130 pmol/cm^2 to 140 pmol/cm^2). This decrease is likely due to edge effects on the gradients during fabrication and is consistent with a decrease in

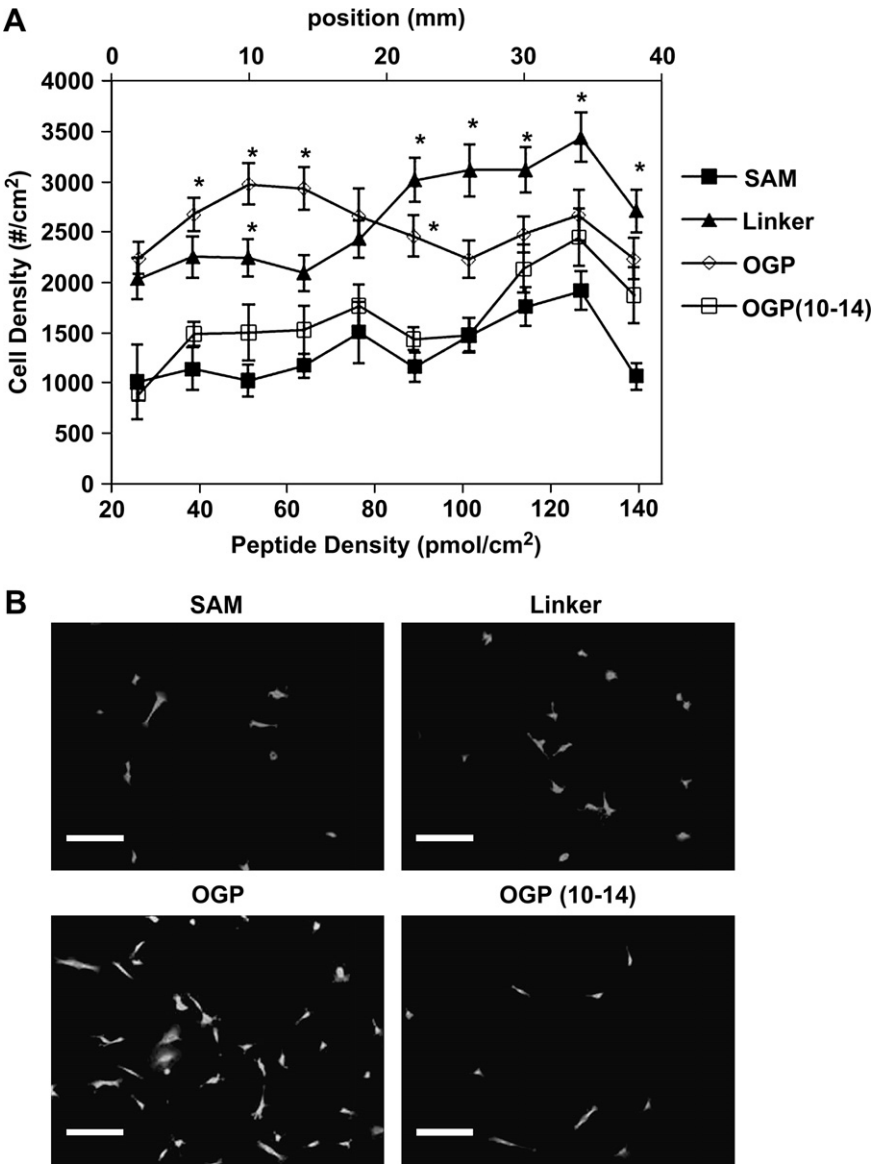

Fig. 3. Cell adhesion of MC3T3-E1 cells on OGP gradient substrates at 4 h post-seeding. (A) Density of cells as a function of peptide density on SAM, linker, and peptide gradient substrates (B) Images of texas red c2 maleimide stained cells on gradients substrates at the 10 mm position (50 pmol/cm^2 peptide density). Scale bars represent 100 μm. * indicates $p < 0.05$ versus SAM gradient substrates. Error bars reflect standard error of the mean.

peptide concentration seen by XPS. There were no differences observed in cell morphology at 4 h between substrates and at different peptide concentrations (data not shown).

3.4. Effect of immobilized OGP concentration on cell proliferation

Cell density and morphology were also measured on peptide gradient substrates at day 3 and day 7 using automated microscopy. For both of these time points, immobilized OGP and immobilized OGP(10-14) had different effects on cell densities. At day 3, OGP gradient substrates had significantly higher cell densities compared to PEO linker gradients at peptide densities 80 pmol/cm^2 to 100 pmol/cm^2 and compared to SAM gradient surfaces at peptide densities 25 pmol/cm^2 to 120 pmol/cm^2. Whereas, immobilized OGP(10-14) peptide only had higher cell densities compared to the SAM gradients at 40 pmol/cm^2 and averaged lower cells densities across the gradient compare to the full peptide (Fig. 4A).

By day 7, differences between OGP gradients and SAM control gradients were no longer observed. The density of MC3T3-E1 cells on OGP gradients and SAM gradients increased slightly with increasing hydrophilicity, ranging from 25,000 cells/cm^2 to 30,000 cells/cm^2 over 35 mm of the gradient. At 30 mm–40 mm positions, OGP and SAM gradient surfaces had higher cell densities on the gradients compared to the linker gradients (Fig. 4B). For the shorter peptide, OGP(10-14), the density of cells on the gradients did not increase with hydrophilicity and remained fairly constant across the gradient within error. These results differed greatly from 4 h and day 3 cell density data.

To characterize cell proliferation as a function of immobilized OGP and OGP(10-14) substrates, the doubling rate of MC3T3-E1 cells was calculated based on day 3 and day 7 cell density data relative to the initial cell seeding concentration. Cell doubling rates were assumed to be constant for each time interval. Immobilized OGP peptide had an impact on cell doubling rate at day 3. The doubling rate was independent of immobilized peptide density, but was less (faster) than the average doubling rates on SAM gradient substrates, PEO linker gradient substrates, tissue culture polystyrene, and glass. Even at the closest point, 40 pmol/cm^2 to 60 pmol/cm^2, the cell

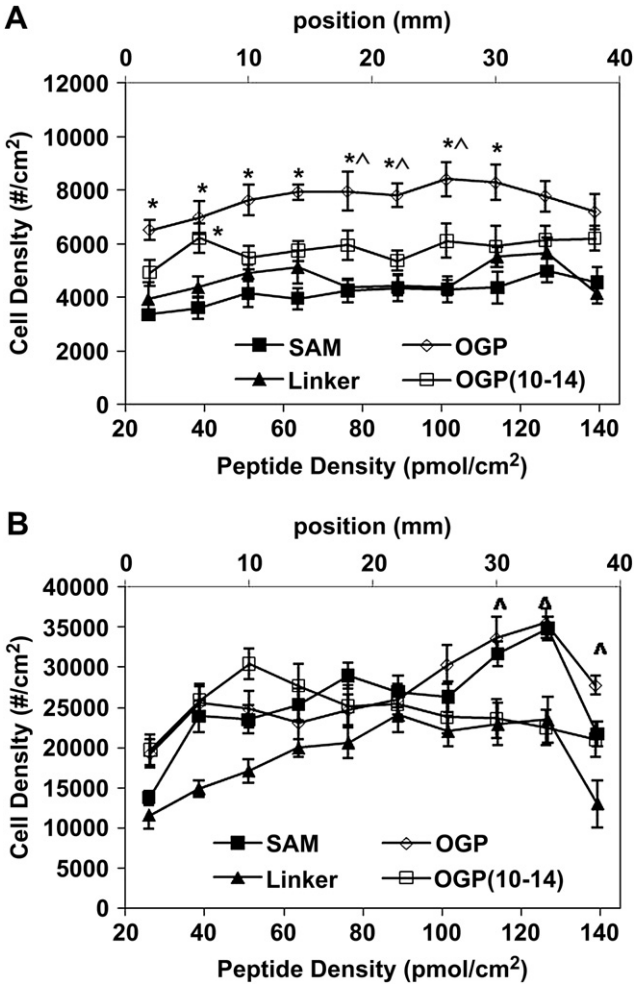

Fig. 4. Cell density as a function of peptide concentration at (A) 3 days and (B) 7 days post-seeding. * indicates $p < 0.05$ versus SAM surface. ^ indicated $p < 0.05$ versus linker surface. Error bars reflect standard error of the mean.

doubling time was at least 35% faster on OGP substrates relative to SAM gradients alone, signifying an increase in cell proliferation. (Fig. 5A) At day 7 time intervals, the doubling rate for MC3T3-E1 cells was not faster on OGP gradient substrates compared to SAM, linker, and OGP(10-14) gradients at all concentrations. Hence, the effect of immobilized OGP peptide on doubling rate of MC3T3-E1 cells was only seen between 0 days and 3 days (Fig. 5B).

3.5. Effect of OGP on gene expression of osteogenic markers

To determine the effect of OGP on gene expression of osteogenic markers in MC3T3-E1 cells, cells were incubated with soluble OGP at similar concentrations used for immobilized peptide in cell adhesion and proliferation experiments, 10^{-7} mol/L. Increases in expression of collagen I mRNA, a preliminary indicator of osteogenic differentiation, were observed in cells treated with OGP and OGP(10-14) (Fig. 6A). Decreases in runx2, an transcription factor associated with osteogenic differentiation, was observed in OGP and OGP(10-14) treated cells which while counter intuitive has been seen previously [23] (Fig. 6B).

4. Discussion

The development of universal substrate gradients for click chemistry cycloaddition of multiple types of peptides has provided a useful platform for exploring the response of cells to immobilized peptide. This study examined the effect of immobilized OGP and the short fragment OGP(10-14) peptide on cell adhesion, morphology and proliferation. Fabrication of the OGP peptide gradients was verified with XPS and contact angle measurements. The results demonstrated reproducible fabrication of linear OGP peptide gradients ranging from 0 pmol/cm^2 to 140 pmol/cm^2. The effects of soluble OGP on osteoblast lineage cells has previously been observed in the range from 10^{-14} mol/L to 10^{-7} mol/L in a biphasic response [6]. The spatial densities of OGP on the substrates fall into this critical range when converted to molar concentrations. Interestingly, previous studies with epidermal growth factor (EGF) have demonstrated that a much smaller concentration of growth factor is required when the growth factor is tethered to the surface rather than soluble in media to induce similar cell response [24]. Hence, it is advantageous to cover a wide range of peptide densities when the bioactive surfaces concentration conditions of immobilized ligand is unknown.

Adhesion of cells to substrates is important for viability and proliferation. As OGP has not been shown to affect adhesion, it was expected that immobilized OGP would not influence the adhesion of MC3T3-E1 cells and that cell adhesion would depend largely on surface energy. Previous studies have demonstrated an increase in

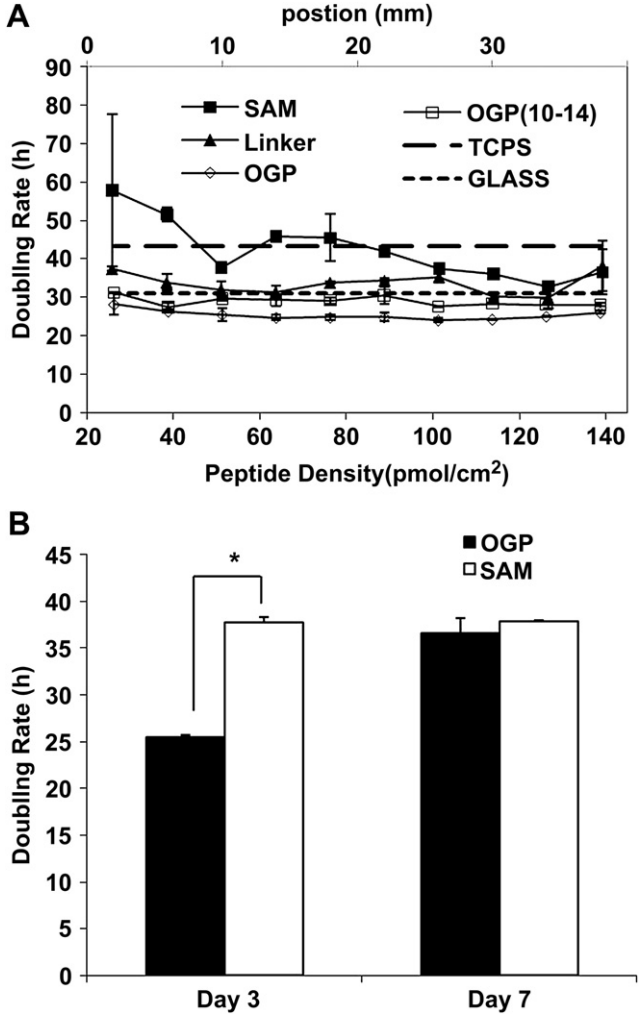

Fig. 5. Doubling rate of MC3T3-E1 cells on gradient surfaces at (A) day 3 and at the (B) 10 mm position for day 2, 3, and 7. Doubling rate represents the time is takes for cells to double in number. * indicates $p < 0.05$ versus SAM surface. Error bars reflect standard error of the mean.

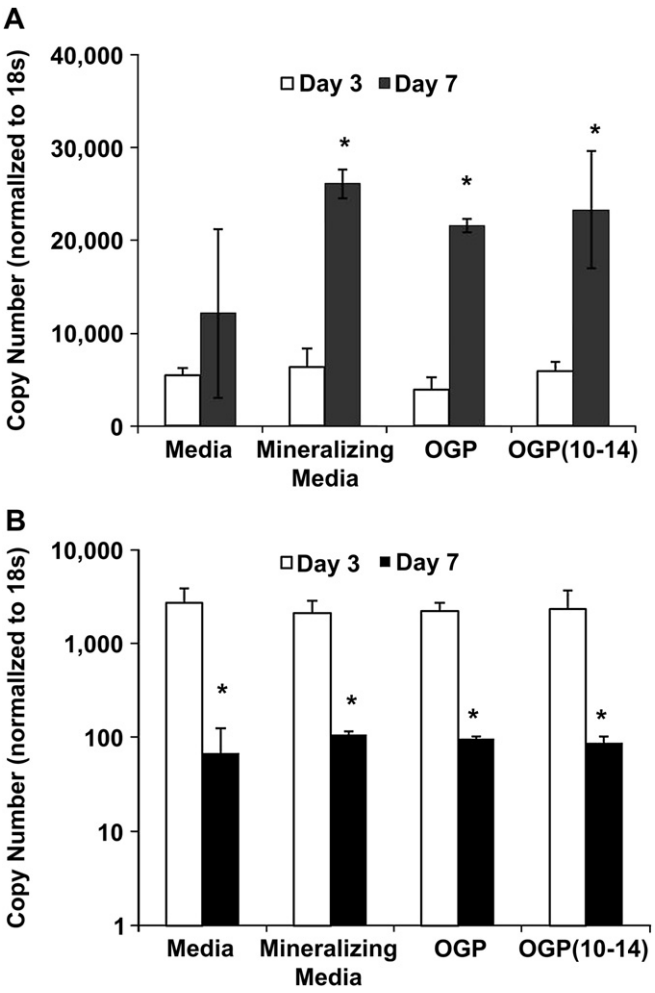

Fig. 6. OGP and OGP(10-14) peptides increased collagen I expression at 7 days post-seeding and did not affect Runx2 expression compared to media control. Real-time RT-PCR was performed on MC3T3-E1 cells grown for 3 and 7 days in the presence of 10^{-7} mol/L OGP or OGP(10-14). 18 S was amplified as a loading control. (A) Analysis of collagen I RNA copy number and (B) Runx2 copy number. * indicates $p < 0.05$ between day 3 and day 7.

cell adhesion with increases in hydrophilicity [19]. However, we found that cell adhesion at 4 h was dependent on OGP peptide concentration and not just on surface energy. Cell adhesion was higher at low peptide concentrations than at higher peptide concentrations. Typically, cell adhesion is regulated through specific integrin receptor interactions and less specific proteoglycan interactions [25]. Because OGP peptide does not contain a known adhesion promoting sequence, such as RGD, which associates with integrin receptors, it is assumed that increased cell adhesion in this region was initiated through non-specific interactions with proteoglycans. OGP peptide has a net positive charge which suggests it might interact electrostatically to negatively charged proteoglycans. The lower concentration of OGP may increase the peptide availability for interacting with the proteoglycans and therefore promote increased cell adhesion. Further, it seems OGP dependent adhesion does not stimulate cell spreading as we did not observe changes in cell spreading of MC3T3-E1 cells on the gradients.

Cell proliferation is the first stage in regeneration of bone tissue and therefore a key step for focus in the analysis of cell–material interactions. The proliferative stage typically occurs during the first 4 weeks of regeneration and is needed to establish a layer of cells for matrix maturation to begin [26]. In this study, cell proliferation was determined based on cell density at various time points and the doubling rate was calculated from these density values assuming a constant rate. The results demonstrated that MC3T3-E1 cells seeded on immobilized OGP had faster doubling rates than cells seeded on control surfaces at 3 days, indicating that immobilized OGP may increase cell proliferation early in the regenerative process. At 7 days, the effect of immobilized OGP on cell proliferation was no longer seen. This is consistent with the model for the developmental pattern of osteoblasts. In osteoblast development, the proliferative phase slows as the expression of cell cycle and cell growth regulated genes are down-regulated and genes associated with maturation of the osteoblast phenotype are upregulated [26]. Decreases in cell proliferation at 7 days on OGP substrates can indicate transition from the proliferative phase to the maturation phase.

Similar to soluble OGP, immobilized OGP increased cell proliferation of osteoblast lineage cells, but the results demonstrated that increases in cell proliferation were independent of immobilized OGP concentration. This result is very different from the biphasic response of cell proliferation observed with different soluble OGP concentrations [6]. This difference observed between soluble and immobilized OGP may be due to two reasons. First, immobilized OGP may only be active when the (10-14) region is cleaved from the substrate surface. Studies have shown that the OGP(10-14) portion is the active region of the peptide that interacts with the cell surface [7]. If cleaved from the substrate, OGP(10-14) peptide will be soluble, subjecting all cells on the gradient to similar OGP(10-14) concentrations. And interestingly, immobilized OGP(10-14), which is not able to be cleaved from the surface, had a lower impact on cell proliferation compared to the full peptide suggesting that the active region does need to be cleaved from the substrate to enhance cell proliferation.

Second, it is known that soluble OGP increases cell proliferation in a biphasic dependent manner, that is indicative of an autocrine/paracrine mode of regulation [6]. In previous studies, the presence of suboptimal and optimal levels of exogenous soluble OGP triggers a 2-fold–5-fold increase in endogenous OGP expressed from osteoblast lineage cells [8]. For immobilized OGP gradient substrates, the effect of immobilized OGP concentration may be overwhelmed by the concentration of soluble endogenous OGP expressed from the cells over time. The expression of soluble OGP from the cells in addition to cleavage of the active OGP region from the substrate makes it difficult to relate immobilized concentration to cell proliferation over time.

For tissue engineering applications, immobilization of growth factors or peptides on tissue engineered substrates is advantageous for promotion of viability, proliferation, and differentiation. The activity of immobilized growth factors and growth factor peptides has been studied previously for epidermal growth factor (EGF), nerve growth factor (NGF), bone morphogenic protein (BMP-2), transforming growth factor (TGF), Sonic hedgehog, and vascular endothelial growth factor (VEGF) [24,27–34]. Typically, bioactivity of immobilized growth factors is longer than that of untethered growth factors, because the growth factors remain in close proximity with cells for longer periods of time when used in vivo [35]. However, this may not be the case for immobilized OGP due to cleavage of the active region and endogenous OGP expression from the cells. Overall, the effect of immobilized OGP is short compared to other immobilized growth factors used in previous literature.

Finally, gene expression of cells on substrate surfaces is typically a good indicator for cell differentiation. Because it is assumed that active OGP is soluble in solution, we measured the gene expression in MC3T3-E1 cells in the presence of soluble OGP at concentrations similar to immobilized OGP on gradient substrates studied. From day 3 to day 7 there was a 10-fold increase in collagen I expression in MC3T3-E1 cells treated with OGP and OGP(10-14), indicating

that the cells are beginning to increase matrix protein expression for the initial stages of bone mineralization [26]. Additionally, there was a decrease in Runx2 mRNA expression which is consistent with previous analysis of mRNA expression of MC3T3-E1 cells during osteoblast differentiation [23]. Both of these expression levels indicate a transition of MC3T3-E1 cells from proliferative phase to matrix maturation from day 3 to day 7.

5. Conclusions

The fabrication of peptide gradient surfaces with click chemistry enabled the characterization of osteoblast response to a wide variation of peptide concentrations on a single substrate. We further demonstrated that the OGP retained its bioactivity when tethered to the substrate. Immobilized OGP increased cell proliferation from 0 to 3 days at all densities indicating it may be useful as a proliferative peptide in future engineered tissue substrates. In addition, the tethered 10-14 OGP fragment also appeared to stimulate proliferation which suggests that the activation sequence is located on the cell surface.

Acknowledgements

This work was supported by a NIST Innovation in Measurement Science Award in Cellular Biometrology (MLB) and a NIST NRC postdoctoral fellowhip (NMM). The authors would like to thank Christopher M. Stafford, Ryan Nieuwendaal, Michael C. Weiger, Khaled A. Aamer, William Wallace, Kathy Flynn for their support of this work.

References

[1] Kuntz RM, Saltzman WM. Neutrophil motility in extracellular matrix gels: mesh size and adhesion affect speed of migration. Biophys J 1997;72:1472–80.
[2] Maheshwari G, Wells A, Griffith LG, Lauffenburger DA. Biophysical integration of effects of epidermal growth factor and fibronectin on fibroblast migration. Biophys J 1999;76:2814–23.
[3] Mapili G, Lu Y, Chen S, Roy K. Laser-layered microfabrication of spatially patterned functionalized tissue-engineering scaffolds. J Biomed Mater Res Part B 2005;75:414–24.
[4] Fan VH, Tamama K, Au A, Littrell R, Richardson LB, Wright JW, et al. Tethered epidermal growth factor provides a survival advantage to mesenchymal stem cells. Stem Cells 2007;25:1241–51.
[5] Bab I, Gazit D, Chorev M, Muhlrad A, Shteyer A, Greenberg Z, et al. Histone H4-related osteogenic growth peptide (OGP): a novel circulating stimulator of osteoblastic activity. EMBO J 1992;11:1867–73.
[6] Greenberg Z, Chorev M, Muhlrad A, Shteyer A, Namdarattar M, Casap N, et al. Structural and functional-characterization of osteogenic growth peptide from human serum – identity with rat and mouse homologs. J Clin Endocrinol Metab 1995;80:2330–5.
[7] Chen ZX, Chang M, Peng YL, Zhao L, Zhan YR, Wang LJ, et al. Osteogenic growth peptide C-terminal pentapeptide [OGP(10-14)] acts on rat bone marrow mesenchymal stem cells to promote differentiation to osteoblasts and to inhibit differentiation to adipocytes. Regul Pept 2007;142:16–23.
[8] Gabarin N, Gavish H, Muhlrad A, Chen YC, Namdar-Attar M, Nissenson RA, et al. Mitogenic G(i) protein-MAP kinase signaling cascade in MC3T3-E1 osteogenic cells: activation by C-terminal pentapeptide of osteogenic growth peptide [OGP(10-14)] and attenuation of activation by cAMP. J Cell Biochem 2001;81:594–603.
[9] Mattii L, Battolla B, Moscato S, Fazzi R, Galimberti S, Bernardini N, et al. The small peptide OGP(10-14) acts through Src kinases and RhoA pathways in Mo-7e cells: morphologic and immunologic evaluation. Med Sci Monit 2008;14:BR103–108.
[10] Mattii L, Fazzi R, Moscato S, Segnani C, Pacini S, Galimberti S, et al. Carboxy-terminal fragment of osteogenic growth peptide regulates myeloid differentiation through RhoA. J Cell Biochem 2004;93:1231–41.
[11] Miguel SM, Namdar-Attar M, Noh T, Frenkel B, Bab I. ERK1/2-activated de novo Mapkapk2 synthesis is essential for osteogenic growth peptide mitogenic signaling in osteoblastic cells. J Biol Chem 2005;280:37495–502.
[12] Gabet Y, Muller R, Regev E, Sela J, Shteyer A, Salisbury K, et al. Osteogenic growth peptide modulates fracture callus structural and mechanical properties. Bone 2004;35:65–73.
[13] Spreafico A, Frediani B, Capperucci C, Leonini A, Gambera D, Ferrata P, et al. Osteogenic growth peptide effects on primary human osteoblast cultures: potential relevance for the treatment of glucocorticoid-induced osteoporosis. J Cell Biochem 2006;98:1007–20.
[14] Horii A, Wang X, Gelain F, Zhang S. Biological designer self-assembling peptide nanofiber scaffolds significantly enhance osteoblast proliferation, differentiation and 3-D migration. PLoS ONE 2007;2:e190.
[15] Shuqiang M, Kunzheng W, Xiaoqiang D, Wei W, Mingyu Z, Daocheng W. Osteogenic growth peptide incorporated into PLGA scaffolds accelerates healing of segmental long bone defects in rabbits. J Plast Reconstr Aesthet Surg 2008;61:1558–60.
[16] Nebhani L, Barner-Kowollik C. Orthogonal transformations on solid substrates: efficient avenues to surface modification. Adv Mater 2009;47(22):6053–71.
[17] Hawker CJ, Wooley KL. The convergence of synthetic organic and polymer chemistries. Science 2005;309:1200–5.
[18] Yousaf MN, Mrksich M. Diels-Alder reaction for the selective immobilization of protein to electroactive self-assembled monolayers. J Am Chem Soc 1999;121:4286–7.
[19] Gallant ND, Lavery KA, Amis EJ, Becker ML. Universal gradient substrates for "click" biofunctionalization. Adv Mater 2007;19:965–9.
[20] Roberson SV, Fahey AJ, Sehgal A, Karim A. Multifunctional ToF-SIMS: combinatorial mapping of gradient energy substrates. Appl Surf Sci 2002;200:150–64.
[21] Fadeev AY, McCarthy TJ. Trialkylsilane monolayers covalently attached to silicon surfaces: wettability studies indicating that molecular topography contributes to contact angle hysteresis. Langmuir 1999;15:3759–66.
[22] Bailey LO, Washburn NR, Simon Jr CG, Chan ES, Wang FW. Quantification of inflammatory cellular responses using real-time polymerase chain reaction. J Biomed Mater Res 2004;69:305–13.
[23] Pregizer S, Baniwal SK, Yan X, Borok Z, Frenkel B. Progressive recruitment of Runx2 to genomic targets despite decreasing expression during osteoblast differentiation. J Cell Biochem 2008;105:965–70.
[24] Chen G, Ito Y, Imanishi Y. Photo-immobilization of epidermal growth factor enhances its mitogenic effect by artificial juxtacrine signaling. Biochim Biophys Acta 1997;1358:200–8.
[25] Plow EF, Haas TA, Zhang L, Loftus J, Smith JW. Ligand binding to integrins 2000:21785–8.
[26] Lian JB, Stein GS. Concepts of osteoblast growth and differentiation: basis for modulation of bone cell development and tissue formation. Crit Rev Oral Biol Med 1992;3:269–305.
[27] Bhang SH, Lee TJ, Yang HS, La WG, Han AM, Kwon YH, et al. Enhanced nerve growth factor efficiency in neural cell culture by immobilization on the culture substrate. Biochem Biophys Res Commun 2009;382:315–20.
[28] Chen PR, Chen MH, Sun JS, Chen MH, Tsai CC, Lin FH. Biocompatibility of NGF-grafted GTG membranes for peripheral nerve repair using cultured Schwann cells. Biomaterials 2004;25:5667–73.
[29] Lim TY, Wang W, Shi Z, Poh CK, Neoh KG. Human bone marrow-derived mesenchymal stem cells and osteoblast differentiation on titanium with surface-grafted chitosan and immobilized bone morphogenetic protein-2. J Mater Sci Mater Med 2009;20:1–10.
[30] Yamachika E, Tsujigiwa H, Shirasu N, Ueno T, Sakata Y, Fukunaga J, et al. Immobilized recombinant human bone morphogenetic protein-2 enhances the phosphorylation of receptor-activated Smads. J Biomed Mater Res 2009;88:599–607.
[31] Metzger W, Grenner N, Motsch SE, Strehlow R, Pohlemann T, Oberringer M. Induction of myofibroblastic differentiation in vitro by covalently immobilized transforming growth factor-beta(1). Tissue Eng 2007;13:2751–60.
[32] Mann BK, Schmedlen RH, West JL. Tethered-TGF-beta increases extracellular matrix production of vascular smooth muscle cells. Biomaterials 2001;22:439–44.
[33] Ho JE, Chung EH, Wall S, Schaffer DV, Healy KE. Immobilized sonic hedgehog N-terminal signaling domain enhances differentiation of bone marrow-derived mesenchymal stem cells. J Biomed Mater Res 2007;83:1200–8.
[34] Backer MV, Patel V, Jehning BT, Claffey KP, Backer JM. Surface immobilization of active vascular endothelial growth factor via a cysteine-containing tag. Biomaterials 2006;27:5452–8.
[35] Stefonek TJ, Masters KS. Immobilized gradients of epidermal growth factor promote accelerated and directed keratinocyte migration. Wound Repair Regen 2007;15:847–55.